Aza-Crown-Capped Porphyrin Models of Myoglobin: Studies of the Steric Interactions of Gas Binding

James P. Collman,*,† Paul C. Herrmann,† Lei Fu,† Todd A. Eberspacher,† Michael Eubanks,† Bernard Boitrel,† Pascal Hayoz, Xumu Zhang,† John I. Brauman,† and Victor W. Day‡

Contribution from the Department of Chemistry, Stanford University, Stanford, California 94305-5080, and Department of Chemistry, University of Nebraska, Lincoln, Nebraska 68588-0304

Received November 13, 1996[⊗]

Abstract: A series of myoglobin active site analogues (**1**−**6**) has been synthesized and characterized. These synthetic models differ in their cavity dimensions, and have been designed to demonstrate the effects of steric factors on O_2 and CO binding affinities. Quantitative gas titrations were employed to measure these affinities, yielding *M* values that are strikingly lower than those reported for hemoglobin and myoglobin. The 1,4,7-triazacyclononane-capped porphyrin **1** has about 1200 times the CO affinity but only about 10 times the O_2 affinity of the cyclam-capped porphyrin **2**, suggesting a more open gas binding cavity for **1**. The cavity dimensions and conformation of **2** were determined by single-crystal X-ray structural analysis of the Zn analogue **7**. This paper unequivocally demonstrates that steric effects can control the ratio of O_2/CO binding constants.

Introduction

Hemoglobin (Hb) and myoglobin (Mb) are the proteins responsible for mammalian dioxygen transport and storage. Both Hb and Mb contain a heme axially bound to a histidine residue, resulting in a 5-coordinate high-spin ($S = 2$) Fe(II) complex. In addition to binding O_2, this 5-coordinate Fe(II) active site binds CO tenaciously. Consequently both proteins are severely inhibited by carbon monoxide.[1]

The *in vivo* production of carbon monoxide during the breakdown of heme by heme oxygenase further complicates dioxygen transport and storage.[2] Exactly one molecule of CO is produced per molecule of heme catabolized, resulting in a partial pressure of CO on the order of 1×10^{-3} Torr at the cellular level.[3] In fact, approximately 1% of a human's Hb is carbonylated due to this *in vivo* CO production. Thus, the heme proteins are designed to transport and store dioxygen in the presence of an endogenous poison, CO.

The nature of the O_2 interaction with Hb has been of interest for some time. Pauling hypothesized in 1964 (and neutron diffraction studies on oxyMb later confirmed) that bound dioxygen is stabilized by a hydrogen bond from the distal histidine residue to the terminal O atom of the bound O_2 molecule.[4] Recently, synthetic models of Hb and Mb have been invaluable in unraveling the subtle complexities of reversible O_2 binding and inhibition by CO.[5] The earliest structurally and functionally sound iron porphyrin model of the Hb and Mb active sites was the "picket fence" porphyrin.[6ab] Dioxygen affinity studies of this model yielded values similar to those exhibited by Hb and Mb. However, the CO affinity of picket fence porphyrin was *ca.* 30 times that of Hb.[6c] If Hb or Mb had the same CO to O_2 affinity ratio (*M* value)[7] as the picket fence porphyrin, mammals would suffocate from their own heme catabolism. Results from synthetic models have been consistent with the hypothesis that the protein moieties of Hb and Mb are large determinants of the protein's *M* value.

On the basis of picket fence models as well as Hb and Mb X-ray crystal structures, it was proposed that the affinity of Hb and Mb for carbon monoxide is decreased by a steric interaction of the linearly bound CO with "distal" amino acid residues in the vicinity of the binding site.[8] Dioxygen, binding in a bent fashion, should be free of such an interaction. Work on the "pocket",[9ab] "hybrid",[9c] "capped" [9d−f] porphyrins provided ad-

† Stanford University.

‡ University of Nebraska.

[⊗] Abstract published in *Advance ACS Abstracts,* April 1, 1997.

(1) (a) Perutz, M. F. *Nature* **1970**, *228*, 726. (b) Perutz, M. F.; Fermi, G.; Luisi, B.; Shaanan, B.; Liddington, R. C. *Acc. Chem. Res.* **1987**, *20*, 309. (c) Perutz, M. F. *Annu. Rev. Biochem.* **1979**, *48*, 327. (d) Perutz, M. F. *Br. Med. Bull.* **1976**, *32*, 195.

(2) Sjostrand, T. *Acta Physiol. Scand.* **1952**, 26, 328.

(3) (a) Metz, G.; Sjostrand, T. *Acta Physiol. Scand.* **1954**, *31*, 334. (b) Coburn, R. F. *Ann. N. Y. Acad. Sci.* **1970**, *174*, 11.

(4) (a) Pauling, L. *Nature* **1964**, *203*, 182. (b) Phillips, S. E. V.; Shoenborn, B. P. *Nature* **1981**, *292*, 81.

(5) For reviews see: (a) Collman, J. P. *Acc. Chem. Res.* **1977**, *10*, 265. (b) Jones, R. D.; Summerville, D. A.; Basolo, F. *Chem. Rev.* **1979**, *79*, 139. (c) Collman, J. P.; Halbert, T. R.; Suslick, K. S. In *Metal Ion Activation of Dioxygen*; Spiro, T. G., Ed.; Wiley: New York, 1980; Chapter 1. (d) Traylor, T. G. *Acc. Chem. Res.* **1981**, *14*, 102. (f) Scheidt, W. R.; Reed, C. A. *Chem. Rev.* **1981**, *81*, 543. (g) Jameson, G. B.; Ibers, J. A. *Comments Inorg. Chem.* **1983**, *2*, 97. (h) Niederhoffer, E. C.; Timmons, J. H.; Martell, A. E. *Chem. Rev.* **1984**, *84*, 7. (i) Baldwin, J. E.; Perlmutter, P. In *Topics in Current Chemistry*; Boschke, F. L., Ed.; Springer: Berlin, 1984; p 181. (l) Suslick, K. S.; Reinert, T. *J. Chem. Educ.* **1985**, *62*, 974. (m) Momenteau, M. *Pure Appl. Chem.* **1986**, *58*, 1493. (n) Momenteau, M.; Reed, C. A. *Chem. Rev.* **1994**, *94*, 659. (o) Jameson, G. B. In *Metal-Containing Polymeric Materials*; Carraher, C., Zeldin, M., Sheats, J., Culbertson, B., Pittman, C. U., Jr., Eds.; Plenum: New York, 1996; p 421.

(6) (a) Collman, J. P.; Gagne, R. R.; Halbert, T. R.; Marchon, J. C.; Reed, C. A. *J. Am. Chem. Soc.* **1973**, *95*, 7868. (b) Collman, J. P.; Gagne, R. R.; Reed, C. A.; Halbert, T. R.; Lang, G.; Robinson, W. T. *J. Am. Chem. Soc.* **1975**, *97*, 1427. (c) Collman, J. P.; Brauman, J. I.; Iverson, B. L.; Sessler, J. L.; Morris, R. M.; Gibson, Q. H. *J. Am. Chem. Soc.* **1983**, *105*, 3052.

(7) $M = K_{CO}/K_{O_2} = P_{1/2}{}^{O_2}/P_{1/2}{}^{CO}$.

(8) (a) Collman, J. P.; Brauman, J. I.; Halbert, T. R.; Suslick, K. S. *Proc. Natl. Acad. Sci. U.S.A.* **1976**, *73*, 3333. (b) Collman, J. P.; Brauman, J. I.; Doxsee, K. M. *Proc. Natl. Acad. Sci. U.S.A.* **1979**, *76*, 6035.

(9) (a) Kim, K.; Fettinger, J.; Sessler, J. K.; Cyr, M.; Hugdahl, J.; Collman, J. P.; Ibers, J. A. *J. Am. Chem. Soc.* **1989**, *111*, 403. (b) Collman, J. P.; Brauman, J. I.; Iverson, B. L.; Sessler, J. L.; Morris, R. M.; Gibson, Q. H. *J. Am. Chem. Soc.* **1983**, *105*, 3052. (c) Tetreau, C.; Lavalette, D.; Momenteau, M.; Fischer, J.; Weiss, R. *J. Am. Chem. Soc.* **1994**, *116*, 11840. (d) Slebodnick, C.; Duval, M. L.; Ibers, J. A. *Inorg. Chem.* **1996**, *35*, 3607. (e) Hashimoto, T.; Dyer, R. T.; Crossley, M. J.; Baldwin, J. E.; Basolo, F. *J. Am. Chem. Soc.* **1982**, *104*, 2101**.** (f) Ross, E.; Boitrel, B.; Quelquejeu, M.; Kossanyi, A. *Tetrahedron Lett.* **1993**, *34*, 7267.

S0002-7863(96)03945-5 CCC: $14.00

ditional evidence for the plausibility of this hypothesis. The decreased size of the gas binding cavity in the pocket porphyrins resulted in *M* values on the order of 200. Infrared spectral studies of these compounds were consistent with a CO more weakly bound than in the case of picket fence porphyrin.

Various X-ray crystallographic studies of CO bound Hb and Mb purported to observe a steric interaction in the CO bound proteins. The CO unit is reported to be tipped off axis, relative to the heme plane normal, from 7° to 47°.[10] Recent interpretation of the available structural data favors a smaller deviation from the heme plane normal.[9d] These recently estimated angles have spawned considerable debate as to whether steric or electrostatic effects play the greater role in determining the CO affinity of Hb and Mb. Spiro *et al*. have suggested that a polar interaction between the terminal oxygen atom of bound CO and the lone pair on the distal histidine plays a substantial role in determining the CO affinity of Mb. They have argued that off-axis bending of the Fe−CO unit, while drastically reducing the strength of the Fe−C bond, is energetically very costly to the protein moiety and hence unlikely.[11] In addition Traylor has demonstrated that the polarity of the environment surrounding the gas binding pocket has a large effect on the *M* value of model complexes. He argued the *M* value in his studies is influenced by an increase in O_2 affinity with negligible change in CO affinity.[12] The presence of water molecules in the binding pocket has also been suggested as contributing to the relative O_2 and CO affinities. The effects of water in the distal pocket have been evaluated in a series of E7 Mb mutants and have been advanced as the water-displacement model.[13] In the present paper we demonstrate that steric effects alone can drastically reduce the carbon monoxide affinity of an iron(II) porphyrin complex and hence its *M* value.

Experimental Section

Materials and Methods. All oxygen sensitive work was performed in a N_2-filled drybox kept at or below 0.5 ppm O_2. All chemicals were purchased commercially (Aldrich, Acros) and used as received unless otherwise noted. Solvents were distilled under a nitrogen or argon atmosphere from the indicated reagents immediately prior to use: methylene chloride (P_2O_5); benzene, tetrahydrofuran, and toluene (sodium/benzophenone ketyl); methanol (Mg). α,α,α,α-Tetrakis(*o*-aminophenyl)porphyrin was prepared according to the literature procedure.[14] ^{1}H NMR and ^{13}C NMR spectra were obtained on a Nicolet WB-300 or a Varian XL-400 spectrometer and referenced to residual proton solvents. Mass spectra were taken at the University of California, San Francisco, Mass Spectrometry Facility. UV−vis spectra were recorded on a Hewlett-Packard 8452A diode array spectrometer. Elemental analysis was performed by Midwest Microlabs (Indianapolis, IN).

Synthesis and Characterization. Michael Acceptor. In an inert atmosphere box, a 500 mL round bottom flask equipped with a stir bar and a rubber stopper was charged with α,α,α,α-tetrakis(*o*-aminophenyl)porphyrin (1.029 g, 1.53 mmol), CH_2Cl_2 (80 mL), and triethylamine (10 mL). Also in the inert atmosphere box, acryloyl chloride (0.6 mL) was dissolved in CH_2Cl_2 (40 mL) and loaded into a 50 mL syringe. The syringe and flask were removed from the box, and the flask was placed under a positive pressure of dry nitrogen. The acryloyl chloride solution was added to the flask via syringe pump at 10 mL/h. The solution was stirred for 24 h, washed with saturated aqueous sodium bicarbonate (4 × 75 mL) and saturated aqueous sodium chloride (1 × 100 mL), dried over sodium sulfate, filtered, and loaded directly onto a flash silica gel column which had been prepared as a CH_2Cl_2 slurry. The product was eluted with 20% acetone/CH_2Cl_2. Upon removal of the solvent, the desired product was obtained (620 mg, 46%). ^{1}H NMR ($CDCl_3$): δ 8.86 (s, 4H); 8.83 (m, 4H); 7.95 (d, J = 7.2 Hz, 4H); 7.88 (t, J = 7.3 Hz, 4H); 7.54 (t, J = 7.4 Hz, 4H); 6.93 (s, 4H); 5.93 (d, J = 16.6 Hz, 4H); 5.04 (m, 8H); 1.54 (s, 4H); 1.25 (br s, 2H) water; −2.77 (s, 2H). MS: *m/e* = 890.9 (M^+) for $C_{56}H_{42}N_8O_4$ (LSIMS). Anal. Calcd for $C_{56}H_{42}N_8O_4 \cdot H_2O$ (water identified by NMR): C, 73.99; H, 4.88; N, 12.33. Found: C, 74.08; H, 4.90; N, 12.08. UV−vis (toluene): λ_{max} 422 (Soret), 516, 548, 588, 644 nm.

Iron Insertion. Iron insertion was performed in an inert atmosphere box. In a typical reaction, a 100 mL round bottom flask equipped with a stir bar and 45 cm Vigreux column was charged with the Michael acceptor porphyrin (140 mg, 0.2 mmol), tetrahydrofuran (50 mL), and 2,6-lutidine (40 drops). The reaction was heated to reflux, and anhydrous $FeBr_2$ (400 mg, 3 mmol) was added. After the reaction was heated at reflux for 12 h, the solvent was removed *in vacuo* and the residue dissolved in tetrahydrofuran/benzene (1:10), filtered through a coarse frit, and loaded directly onto an alumina column (activity I neutral, 1 cm × 10 cm). The product was eluted with methanol/tetrahydrofuran/benzene (1:1:10). Upon removal of solvent *in vacuo*, the solid product iron(II) Michael acceptor was obtained (130 mg, 87%). MS: *m/e* = 944.2 (M^+) for $C_{56}H_{40}N_8O_4Fe$ (LSIMS). UV−vis (toluene): λ_{max} 418, 422 (split Soret), 538 nm.

Four-Nitrogen Aza-crown-Capped Porphyrin Syntheses. The Michael acceptor (free base or iron(II) derivative) was allowed to react with cyclen or cyclam aza-crown ethers. The conditions under which it was performed were identical, with the exception that the free base reactions were carried out under nitrogen while the syntheses using the Fe(II)-metalated porphyrin were done in a drybox. In a typical reaction, Michael acceptor (0.15 mmol) is dissolved in CH_3OH/CH_2Cl_2 (25:1, 25 mL) in a 50 mL round bottom flask with a stir bar, an aza-crown ether (0.75 mmol) added, and the solution heated to reflux. After 72 h the solution is cooled and the solvent removed *in vacuo*. The resulting solid is dissolved in a minimum amount of CH_2Cl_2 and loaded directly onto an alumina column (activity I neutral, 1 cm × 10 cm). The product is eluted with 2% CH_3OH/CH_2Cl_2. Evaporation of the solvent yields the desired product.

Cyclam-Capped Porphyrin Free Base. Yield: 91%. ^{1}H NMR ($CDCl_3$): δ 10.1 (s, 4H); 8.95 (d, J = 8.4 Hz, 4H); 8.81 (s, 4H); 8.78 (s, 4H); 7.77 (t, J = 7.3 Hz, 4H); 7.49 (d, J = 6.5 Hz, 4H); 7.30 (t, J = 7.4 Hz, 4H); 2.18 (br m, 8H); 2.05 (br s, 8H); 0.3 (br s, 8H); −0.2 (br, 4H); −0.5 (br, 4H); −2.2 (br, 2H); −2.5 (br, 2H); −2.76 (s, 2H). ^{13}C NMR ($CDCl_3$): δ 171; 138; 137; 133; 131; 130; 129; 122; 121; 117; 51; 49; 41; 34; 19. MS: *m/e* = 1091.5 (M^+) for $C_{66}H_{66}N_{12}O_4$ (LSIMS). Anal. Calcd for $C_{66}H_{66}N_{12}O_4 \cdot CH_2Cl_2$: C, 68.46; N, 14.31; H, 5.84. Found: C, 68.12; N, 14.02; H, 5.76. UV−vis (toluene): λ_{max} 426 (Soret), 516, 550, 590, 646 nm.

Cyclen-Capped Porphyrin Free Base. Yield: 70%. ^{1}H NMR ($CDCl_3$): δ 9.55 (s, 4H); 8.88 (d, J = 8.1 Hz, 4H); 8.83 (s, 8H); 7.87 (d, J = 7.3 Hz, 4H); 7.83 (t, J = 7.4 Hz, 4H); 7.44 (t, J = 7.3 Hz, 4H); 1.99 (s, br, 8H); 1.77 (s, br, 8H); 1.4−0.0 (br region, 8H); 1.25 (br, 6H) water; −0.5 to −1.5 (br peak, 4H); −2.73 (s, 2H); −3 to −3.6 (br peak, 4H). MS: *m/e* = 1063.6 (M^+) for $C_{64}H_{62}N_{12}O_4$ (LSIMS). Anal. Calcd for $C_{64}H_{62}N_{12}O_4 \cdot 3H_2O$ (water identified in NMR): C, 68.80; N, 15.04; H, 6.15. Found: C, 69.29; N, 15.06; H, 5.79. UV−vis (toluene): λ_{max} 422 (Soret), 514, 546, 590, 642 nm.

Three-Nitrogen Aza-crown Porphyrin Capping Synthesis. The synthesis is identical to that of the four-nitrogen aza-crown porphyrin capping synthesis described above, except 1.1 equiv of the three-nitrogen aza-crown was used rather than 6 equiv as in the case of the four-nitrogen models.

(10) (a) Heidner, E. J.; Ledner, R. C.; Perutz, M. F. *J. Mol. Biol.* **1976**, *104*, 707. (b) Kuriyan, J.; Wilz, S.; Karplus, M.; Petsko, G. A. *J. Mol. Biol.* **1986**, *192*, 133. (c) Teng, T. -Y.; Srajer, V.; Moffat, K. *Nat. Struct. Biol.* **1994**, *1*, 701. (d) Cheng, X.; Schoenborn, B. P. *J. Mol. Biol.* **1991**, *220*, 381. (e) Quillin, M. L.; Arduini, R. M.; Olson, J. S.; Phillips, Jr. *J. Mol. Biol.* **1993**, *234*, 140. (f) Schlichting, I.; Berendzen, J.; Phillips Jr.; Sweet, R. M. *Nature* **1994**, *371*, 808. (g) Ivanov, D.; Sage, J. T.; Keim, M.; Powel, J. R.; Asher, S. A.; Champion, P. M. *J. Am. Chem. Soc.* **1994**, *116*, 4139. (h) Derenenda, Z.; Dodsong.; Elmsley, P.; Harris, D.; Nagai, K.; Perutz, M. F.; Reanud, J. P. *J. Mol. Biol.* **1990**, *211*, 515. (i) Lim, M.; Jackson, T. A.; Anfinrud, P. A. *Science* **1995**, *269*, 962.

(11) (a) Ray, G. B.; Li, X.-Y.; Ibers, J. A.; Sessler, J. L.; Spiro, T. G. *J. Am. Chem. Soc.* **1994**, *116*, 162. (b) Spiro, T. G. *Science* **1995**, *270*, 221.

(12) (a) Traylor, T. G. *Acc. Chem. Res.* **1981**, *14*, 102. (b) Traylor, T. G.; Koga, N.; Dearduff, L. A. *J. Am. Chem. Soc.* **1985**, *107*, 6504.

(13) Springer, B. A.; Sligar, S. G.; Olson, J. S.; Phillips, G. N. *Chem. Rev.* **1994**, *94*, 699.

(14) (a) Linsey, I. *J. Org. Chem.* **1980**, *45*, 5215. (b) Elliot, C. M. *Anal. Chem.* **1980**, *52*, 666.

1,4,7-Triazacyclononane-Capped Porphyrin Free Base. Yield: 54%. ^{1}H NMR ($CDCl_3$): δ 10.2 (s, 2H); 8.88−8.73 (m, 8H); 8.50 (d, J = 8.1 Hz, 2H); 8.43 (d, J = 8.1 Hz, 2H); 7.9−7.5 (m, 4H); 7.65 (t, J = 7.3 Hz, 2H); 7.6−7.2 (br region, 6H); 6.0 (br, 1H); 5.1 (br, 2H); 2.1 (s, 2H); 1.9 (s, 2H); 1.7−1.4 (br m, 8H); 1.2 (m, 6H); 0.8 (m, 2H); 0.4 (br, 2H); −1.2 (br, 2H); −2.4 (s, 2H); −2.8 (br, 2H). MS: m/e = 1020.5 (M^+) for $C_{62}H_{57}N_{11}O_4$. Anal. Calcd for $C_{62}H_{57}N_{11}O_4 \cdot CH_2Cl_2 \cdot 1H_2O$: C, 67.37; N, 13.72; H, 5.47. Found: C, 67.80; N, 13.67; H, 5.40. UV−vis (toluene): λ_{max} 424 (Soret), 518, 552, 592, 650 nm.

CuBr Insertion. The porphyrin was dissolved in acetonitrile and heated at reflux. Twenty mole equivalents of CuBr was added, and the solution was left at reflux for 24 h. The solution was then cooled to room temperature, solvent removed under vacuum, and the resulting solid suspended in CH_2Cl_2. The suspension was filtered through a fine frit with a 2 cm Celite pad. The filtrate, now free of excess CuBr, was pumped dry under vacuum.

Synthesis of Tailed 1,4,7-Triazacyclononane-Capped Porphyrin. 1,4,7-Triazacyclononane-capped porphyrin was dissolved in methanol, 3-(aminomethyl)pyridine (1.2 equiv) was added, and the solution was heated at reflux for 24 h. The reaction mixture was cooled and the solvent pumped off under vacuum. The resulting solid was dissolved in benzene, loaded onto a neutral activity I alumina column, and eluted with 2% methanol in benzene. The solvent was removed under vacuum, yielding the desired compound.

1,4,7-Triazacyclononane-Capped Pyridine-Tailed Porphyrin Free Base. MS: m/e = 1128.4 (MH^+) for $C_{68}H_{63}N_{13}O_4$ (LSIMS).

Iron(II)-Metalated 1,4,7-Triazacyclononane-Capped Porphyrin 1. ^{1}H NMR (pyridine--d_5): δ 45−50 (m); characteristic of β-pyrrolic protons on a paramagnetic 5-coordinate iron (S = 2) porphyrin. MS: m/e = 1074.3 (M^+) for $C_{62}H_{57}N_{11}O_4Fe$ (LSIMS). UV−vis (toluene): λ_{max} 420, 448 (split Soret), 538 nm. UV−vis (toluene, 1000 equiv of 1,2-dimethylimidazole): λ_{max} 444 (Soret), 566 nm.

Iron(II)-Metalated Cyclam-Capped Porphyrin 2. ^{1}H NMR (pyridine-d_5): δ 49 (s); 51 (s); characteristic of β-pyrrolic protons on a paramagnetic 5-coordinate iron (S = 2) porphyrin. MS: m/e = 1145.5 (M^+) for $C_{66}H_{64}N_{12}O_4Fe$ (LSIMS). UV−vis (toluene): λ_{max} 420, 448 (split Soret), 538 nm. UV−vis (toluene, 1000 equiv of 1,2-dimethylimidazole): λ_{max} 444 (Soret), 566 nm. The sample was exposed to oxygen, and the resulting μ-oxo iron(III) dimer was precipitated from benzene/methanol/THF and sent for elemental analysis. Anal. Calcd for $(FeC_{62}H_{57}N_{11}O_4)_2O \cdot 2$benzene: C, 70.24; N, 13.65; H, 5.73. Found: C, 69.92; N, 13.43; H, 5.68.

Iron(II)-Metalated Cyclen-Capped Porphyrin 3. UV−vis (toluene): λ_{max} 420, 448 (split Soret), 538 nm. UV−vis (toluene, 1000 equiv of 1,2-dimethylimidazole): λ_{max} 444 (Soret), 566 nm.

Iron(II)-Metalated CuBr 1,4,7-Triazacyclononane-Capped Porphyrin 4. ^{1}H NMR (pyridine-d_5): δ 45−50 (m); characteristic of β-pyrrolic protons on a paramagnetic 5-coordinate iron (S = 2) porphyrin. MS: m/e = 1217.3 (M^+) for $C_{62}H_{57}N_{11}O_4FeCuBrO_2$ (LSIMS). The spectra matched the calculated isotope distribution exactly. UV−vis (toluene): λ_{max} 420, 448 (split Soret), 538 nm. UV−vis (toluene, 1000 equiv of 1,2-dimethylimidazole): λ_{max} 444 (Soret), 566 nm.

Iron(II)-Metalated 1,4,7-Triazacyclononane-Capped Pyridine-Tailed Porphyrin 5. MS: m/e = 1182.6 (MH^+) for $C_{68}H_{63}N_{13}O_4Fe$ (LSIMS). UV−vis (toluene): λ_{max} 444 (Soret), 566 nm.

Iron(II)-Metalated CuBr 1,4,7-Triazacyclononane-Capped Pyridine-Tailed Porphyrin 6. UV−vis (toluene): λ_{max} 444 (Soret), 566 nm.

Zinc(II) Cyclam-Capped Porphyrin 7. A 100 mL flask is charged with methanol (30 mL) and Michael acceptor porphyrin (100 mg) and heated at 50 °C for 2 h. The solvent is removed *in vacuo* and the resulting solid dissolved in methylene chloride, placed directly onto a silica column (1 cm × 15 cm), and eluted with chloroform/methanol (20:1). The Zn(II) Michael acceptor is capped according to the procedure described above. ^{1}H NMR (CD_2Cl_2): δ 8.70 (d, 8 H); 8.75 (d, 4H); 7.70 (t, 4H); 7.50 (d, 4H); 7.270 (t, 4H); 1.95−2.05 (br m, 28H); 0.20 (br m, 8H); −0.5 (br s, 4H).

X-ray Crystal Structure Determination of Zinc Cyclam-Capped Porphyrin. Single crystals of $H_2O/CH_3OH/CH_2Cl_2$-solvated Zn(cyclam-capped porphyrin)(OH_2) (**7**) are, at 20 ± 1 °C, monoclinic, space group $C_{2/c}$−C_{2h}^6 (no. 15), with a = 47.088(7) Å, b = 12.606(2) Å, c = 22.501(4) Å, β = 103.821(7)°, V = 12970(4) Å^3, and Z = 8 {d_{calcd} = 1.369 g/cm^3; μ_a(Mo Kα) = 0.45 mm^{-1}}. A full hemisphere of diffracted intensities (1270 10 s frames with an ω scan width of 0.30°) was measured to 0.90 Å resolution using graphite-monochromated Mo Kα radiation on a Siemens SMART CCD area detector. X-rays were provided by a normal focus sealed X-ray tube operated at 50 kV and 40 mA. Lattice constants were determined with the Siemens SMART software package using peak centers for 50 reflections. A total of 24461 integrated reflection intensities having 2θ (Mo Kα) < 46.51° were obtained using the Siemens program SAINT. A total of 9185 of these were independent and gave R_{int} = 0.038. The Siemens SHELXTL-PC software package was used to solve the structure using the "heavy atom" technique and to conduct initial least-squares refinements using F_o data. The final stages of weighted full-matrix least-squares refinement were conducted using F_o^2 data and the SHELTXTL Version 5 software package and converged to give R_1(unweighted, based on F) = 0.052 for 7466 independent reflections having 2θ (Mo Kα) < 46.51° and $I > 2\sigma(I)$ and wR_2(weighted, based on F^2) = 0.131 for 8894 independent reflections having 2θ (Mo Kα) < 46.51° and $I > 0$. The structural model incorporated anisotropic thermal parameters for all non-hydrogen atoms and isotropic thermal parameters for all included hydrogen atoms. Several of the water and methanol solvent molecules of crystallization are disordered. The hydrogen atoms bonded to carbons of the porphyrin ligand were included in the structural model at idealized sp^2- or sp^3-hybridized positions using a C−H bond length of 0.96 Å with their isotropic thermal parameters fixed at values 1.2 times the equivalent isotropic thermal parameters of the carbon atom to which they are bonded. Hydrogen atoms bonded to the four amide nitrogens of the porphyrin ligand and the hydrogens on the coordinated water molecule were located from difference Fourier synthesis and included in the least-squares refinement cycles as independent isotropic atoms. Although hydrogens bonded to the oxygen (O_{2W}) for one of the lattice water molecules could be located from a difference Fourier synthesis, they could not be satisfactorily refined as independent isotropic atoms. These two hydrogens were therefore included in the structural model with the coordinates fixed at the Fourier values and isotropic thermal parameters fixed at values which were 1.2 times the equivalent isotropic thermal parameter of oxygen atom O_{2W}. Hydrogen atoms on the remainder of the solvent molecules of crystallization were not located or included in the structural model.

Results and Discussion

A series of porphyrins (**1**−**6**, Figure 1) were synthesized according to the "congruent multiple Michael addition" method previously reported.[15] Carbon monoxide and dioxygen gas binding to their Fe(II) derivatives was studied preliminarily by ^{1}H NMR spectroscopy in pyridine-d_5, which acts as both the solvent and the axial ligand. After the spectrum indicative of a 5-coordinate iron(II) species was recorded, the sample was exposed to CO or O_2 and a second spectrum recorded. The 5-coordinate porphyrin-bound iron(II) is high-spin and has an NMR spectrum indicative of a paramagnetic S = 2 ground state as evidenced by β-pyrrolic proton signals at ca. 45−55 ppm downfield relative to TMS. When CO or O_2 binds to iron, the resulting complexes are diamagnetic and the NMR spectra are characteristic of an S = 0 system.[16] Typical spectra are shown in Figure 2. The results lead to the important conclusion that the cyclam-capped porphyrin **2** has no detectable affinity for CO at pressures up to 1 atm!

(15) Collman, J. P.; Zhang, X; Herrmann, P. C.; Uffelman, E. S.; Boitrel, B; Straumanis, A; Brauman, J. I. *J. Am. Chem. Soc.* **1994**, *116*, 2681.

(16) (a) LaMar, G. N.; Eaton, G. R.; Holm, R. H.; Walker, F. A. *J. Am. Chem. Soc*. **1973**, *95*, 63. (b) LaMar, G, N.; Walker, F. A. *J. Am. Chem. Soc.* **1973**, *95*, 1782. (c) Goff, H.; LaMar, G. N.; Reed, C. A. *J. Am. Chem. Soc*. **1977**, *99*, 3641. (d) Goff, H.; LaMar, G. N. *J. Am. Chem. Soc.* **1977**, *99*, 6599. (e) Collman, J. P.; Brauman, J. I.; Collins, T. J.; Iverson, B. L.; Lang, G.; Pettman, R. B.; Sessler, J. L.; Walter, M. A. *J. Am. Chem. Soc.* **1983**, *105*, 3038. (f) A sharp diamagnetic ^{1}H NMR spectrum at room temperature is probably the quintessential criterion of a pure iron(II) dioxygen complex: Collman, J. P.; Brauman, J. I.; Doxsee, K. M.; Halbert, T. R.; Bunnenberg, E.; Linder, R. E.; LaMar, G. N.; Del Gaudio, J.; Lang, G.; Spartalian, K. *J. Am. Chem. Soc.* **1980**, *102*, 4182.

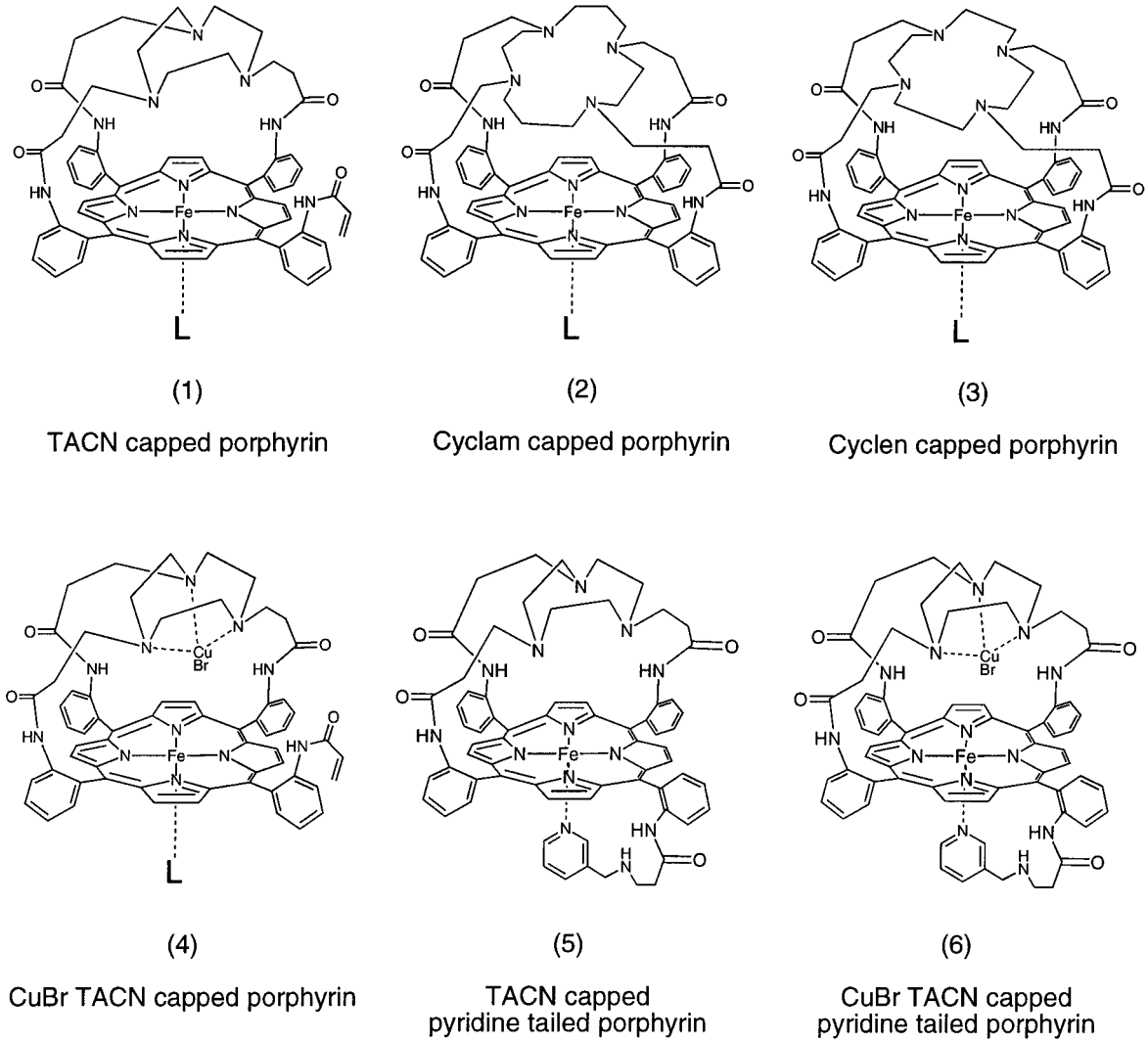

Figure 1. Chemical structures of the compounds referred to in the text. An R-state model results when L = 1,5-dicyclohexylimidazole, and a T-state model results from L = 1,2-dimethylimidazole.

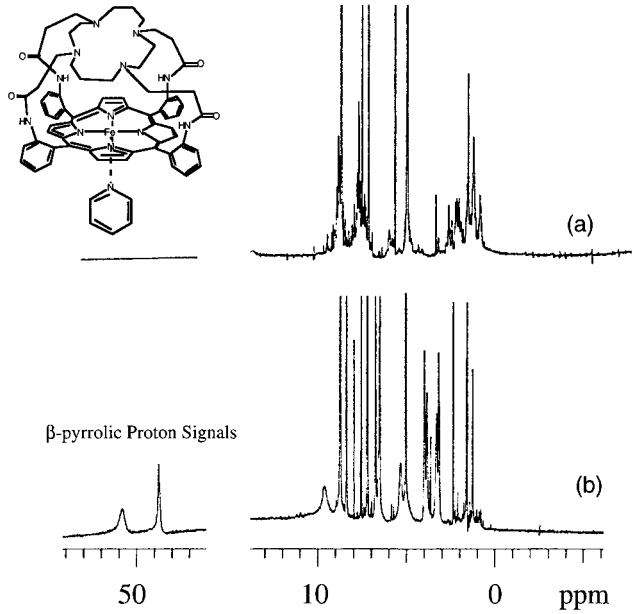

Figure 2. ^{1}H NMR spectra of O_2 bound (a) and O_2-free (b) complexes of compound **2** in pyridine-d_5. Spectra are typical of compounds **1**−**6**. Note the absence of β-pyrrolic proton signals in (a).

Dioxygen and carbon monoxide binding affinity values were determined using a tonometer and UV−vis spectroscopy.[17] Typical data are shown in Figure 3. Ten micromolar porphyrin solutions in toluene with 1000 molar equivalents of axial ligand were titrated with pure O_2 and CO. The resulting $P_{1/2}$ and M values are tabulated in Table 1 along with literature values for Hb, Mb, and pertinent model porphyrin complexes. Carbon monoxide pressures greater than 1 atm were not employed; thus, the reported M values represent a lower limit for the cyclam (**2**) and cyclen (**3**) capped porphyrins. Even though a very large excess of axial ligand was used, the iron(II) remained 5-coordinate until addition of O_2 or CO, because the macrocycle−porphyrin cavity excludes imidazole bases, and thus the formation of a 6-coordinate Fe(II) complex. In addition, the oxygenated (carbonylated) species are stable in solution, for over 10 days.

The M values reported in Table 1 are similar whether the axial ligand is 1,5-dicyclohexylimidazole (1,5-DCIm), 1,2-dimethylimidazole (1,2-Me_2Im), or a covalently attached pyridine tail. Pyridine has a different trans labilizing influence on Fe than does imidazole.[18] Hence, pyridine acts very differently as an axial ligand than imidazole. Even though the affinity of

(17) (a) Rose, N.; Drago, R. S. *J. Am. Chem. Soc.* **1959**, *81*, 6138. (b) Beugelsdijk, T. J.; Drago, R. S. *J. Am. Chem. Soc.* **1975**, *97*, 6466. (c) Collman, J. P.; Brauman, J. I.; Suslick, K. S. *J. Am. Chem. Soc.* **1975**, *97*, 7185.

(18) (a) Rougee, M.; Brault, D. *Biochemistry* **1975**, *18*, 4100. (b) Collman, J. P.; Brauman, J. I.; Doxsee, K. M.; Sessler, J. L.; Morris, R. M.; Gibson, Q. H. *Inorg. Chem.* **1983**, *22*, 1427.

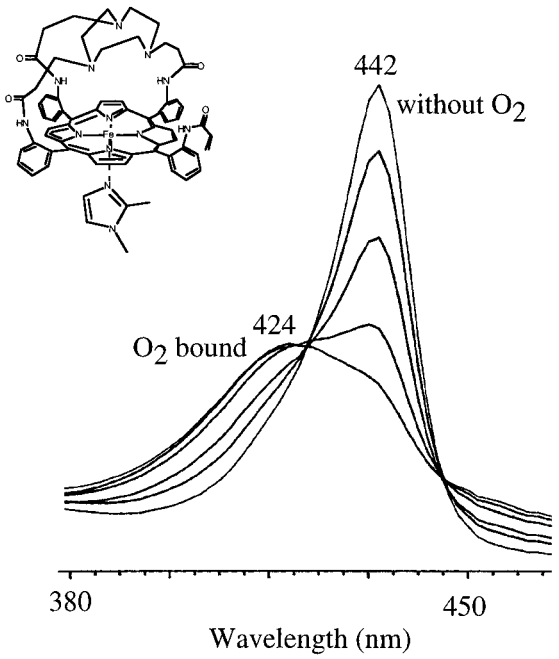

Figure 3. UV−vis spectra of O_2-free and O_2 bound compound **1** with 1000 equiv of 1,2-dimethylimidazole in toluene. Spectra are typical of compounds **1**−**6**.

the Fe for the axial ligand is almost identical for pyridine and imidazole, the observed insensitivity of the *M* value to the axial ligand suggests that the *M* value is predominantly determined by the porphyrin cavity structure.

Also interesting is the relatively small 7-fold increase in O_2 binding affinity on changing from 1,2-Me_2Im (T-state model) to 1,5-DCIm (R-state model) as the axial ligand for compound **2**. Most reported model complexes demonstrate a 10−100-fold increase under the same conditions.[19] The 10-fold effect observed for picket fence porphyrin has been attributed to the geometric relationship of the Fe to the porphyrin plane (see Figure 4). Upon O_2 binding in the T-state picket fence model, the Fe atom is not permitted to become coplanar with the porphyrin. Instead, the Fe atom is forced to remain slightly on the proximal side of the porphyrin away from the bound O_2.[20] The R-state picket fence model on the other hand permits the Fe atom to be in the plane of the porphyrin.

In the aza-crown-capped models, however, an R-state axial ligand which permits the Fe to be coplanar with the porphyrin would require the terminal end of the bound O_2 molecule to extend out, closer to the cap. While the Fe geometry of an R-state model increases the affinity of the Fe for O_2, the terminal end of the bound gas molecule in these models would be forced closer to the cap where it could be sterically destabilized.

Such steric interactions with the intrisically linear CO group appeared to be the origin of the differing *M* values in Table 1. Consequently, a more detailed structural understanding of cavity dimensions for these aza-crown models was needed. Since zinc

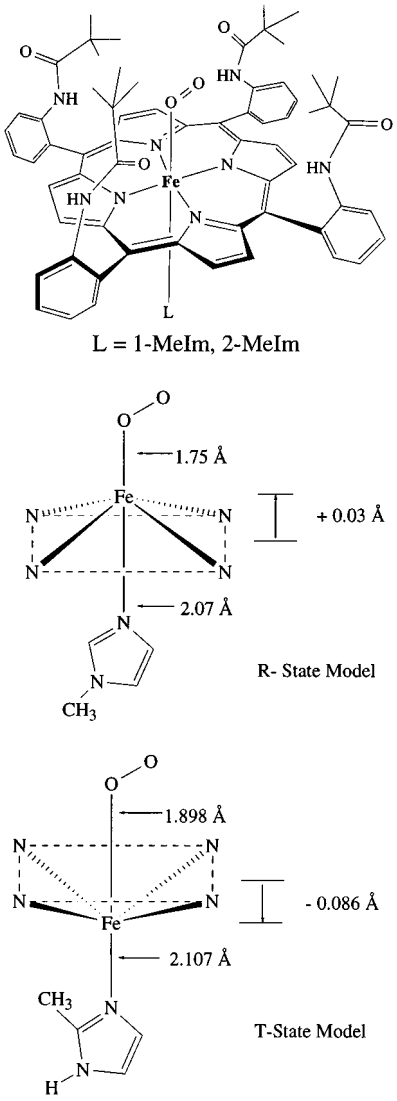

Figure 4. Selected dimensions of R- and T-state picket fence porphyrin complexes as determined by X-ray crystallography. See ref 19 for more details.

porphyrins are easier to crystallize than iron porphyrins and because zinc porphyrin complexes are air and moisture stable, the Zn analogue of **2** (**7**) was synthesized. X-ray quality crystals of **7** were obtained by vapor diffusion of isopropyl alcohol into a saturated solution of **7** [CH_2Cl_2/CH_3OH (3:1)] at room temperature.

A single-crystal X-ray structural analysis of **7** (Figure 5) revealed that it was composed of discrete molecules of the aquo zinc analogue of **2** with H_2O, MeOH, and/or dichloromethane solvent molecules of crystallization surrounding it in the lattice. The Zn^{2+} ion is 5-coordinate, with the pyrrole nitrogens of the porphyrin macrocycle occupying the four basal sites and the oxygen (O_{1W}) of a coordinated water molecule occupying the axial site of a square pyramid. The four pyrrole nitrogens are coplanar to within 0.004 Å, and the Zn atom is displaced from their least-squares mean plane by 0.336 Å toward the apical oxygen which is on the unhindered (proximal) side of the porphyrin. The cyclam cap is attached through its nitrogens to the distal side of the porphyrin by *N*-phenylacrylamide bridges to the *meso*-methine carbons of the porphyrin core. By linking the two macrocycles in this fashion, one might expect to produce an approximately staggered arrangement for the two sets of four (pyrrole or amine) nitrogens. The conformation actually observed is one midway between staggered and eclipsed. This

(19) Appleby, C. E.; Blumberg, W. E.; Bradbury, J. H.; Fuchsman, W. H.; Peisach, J.; Wittenberg, B. A.; Wittenberg, J. B.; Wright, P. E. In *Hemoglobin and Oxygen Binding*; Ho, C., Ed.; North-Holland: Amsterdam, 1982; p 435.

(20) (a) Collman, J. P.; Gagne, R. R.; Reed, C. A.; Robinson, W. T.; Rodley, C. A. *Proc. Natl. Acad. Sci. U.S.A.* **1974**, *71*, 1326. (b) Jameson, G. B.; Molinaro, F.; Ibers, J. A.; Collman, J. P.; Brauman, J. I.; Rose, E.; Suslick, K. S. *J. Am. Chem. Soc.* **1980**, *102*, 3224. (c) Jameson, G. B.; Rodley, G. A.; Robinson, W. T.; Gagne, R. R.; Reed, C. A.; Collman, J. P. *Inorg. Chem.* **1978**, *17*, 850. (d) Jameson, G. B.; Molinaro, F. S.; Ibers, J. A.; Collman, J. P.; Brauman, J. I.; Rose, E.; Suslick, K. S. *J. Am. Chem. Soc.* **1978**, *100*, 6769. (e) Collman, J. P.; Reed, C. A. *J. Am. Chem. Soc.* **1973**, *95*, 2048.

Table 1. Gas Binding Data for Compounds **1**−**6** and Related Compounds of Interest from the Literature[a]

	$P_{1/2}(O_2)$ (Torr)	$P_{1/2}(CO)$ (Torr)	M ($P_{1/2}(O_2)/P_{1/2}(CO)$)	bound CO stretching frequency (cm^{-1})
		T-State Model		
Hb(T)[b]	40	0.3	135[c]	
Fe(picket fence) (1,2-Me_2Im)	38	0.0089	4280[d]	
Fe(4-atom-linked cap) (1-MeIm)	280	100	2.8[e]	
1 (1,2-Me_2Im)	2.3	2.9	0.79	1956
2 (1,2-Me_2Im)	22	>3500	<0.006	
3 (1,2-Me_2Im)	760	>3500	<0.22 at 4 °C	
4 (1,2-Me_2Im)	irreversible	5.9	NA	1965
		R-State Model		
Hb(R)[b]	0.22	0.0014	150[c]	
Mb[b]	0.37−1	0.014−0.025	20−40[f]	
1 (1,5-DCIm)	<0.2			
2 (1,5-DCIm)	∼3	>3500	<0.003	
3 (1,5-DCIm)	∼760	>3500	<0.22	
4 (1,5-DCIm)	irreversible	3.6	NA	
		Pyridine-Tailed Compounds		
5	3.7	1.5	2.47	
6	irreversible	2.8	NA	

[a] Note all data were obtained at 25 °C except the T-state compound **3** which was measured at 4 °C. [b] Measured in H_2O at pH 7. [c] Sharma, V. S.; Schmidt, M. R.; Ranney, H. M. *J. Biol. Chem.* **1976**, *251*, 4267. Steinmeier, R. C.; Parkhurst, L. J. *Biochemistry* **1975**, *14*, 1564. [d] Collman, J. P.; Brauman, J. I.; Inverson, B. L.; Sessler, J. L.; Morris, R. M.; Gibson, Q. H. *J. Am. Chem. Soc.* **1983**, *105*, 3052. [e] Johnson, M. R.; Seok, W. K.; Ibers, J. A. *J. Am. Chem. Soc.* **1991**, *113*, 3998. [f] LaGow, J.; Parkhurst, L. *J. Biochemistry* **1972**, *11*, 4520.

can be seen in Figure 5a and by the facts that the Zn, C_{10}, C_{20}, N_{31}, and N_{38} atoms are coplanar to within 0.03 Å but the Zn, C_5, C_{15}, N_{28}, and N_{35} atoms have the following displacements from their least-squares mean plane: 0.01, −0.41, 0.40, 0.46, and −0.45 Å. This arrangement has one diagonal of the rectangular array of four cyclam nitrogens aligned parallel to one diagonal of the square array of four pyrrole nitrogens and reduces the number of symmetry elements for possibly relating the non-hydrogen atoms of **7**. Although the non-hydrogen atoms of **7** could ideally be related by C_{2v} symmetry, only C_2 symmetry is approximated in the crystal, with the pseudo-C_2 axis passing through the Zn atom, the oxygen atom of the coordinated water molecule, and the centers of gravity for the four coordinated pyrrole nitrogens and the four amine nitrogens of the cyclam cap.

Although **7** does not bind O_2 or CO, it should be a reasonable structural analogue of the 5-coordinate deoxygenated high-spin iron(II) cyclam-capped porphyrin. The average $Zn-N_p$[21] bond length is 2.069 (5, 3, 3, 4) Å,[22] the Zn−O bond length is 2.092(4) Å, and the $Zn-C_t$[23] and C_t-N_p distances are 0.336 and 2.041 (−, 3, 5, 4) Å, respectively. These values are close to those observed for similar bonds in other 5-coordinate zinc(II) porphyrin complexes,[24] and to those of high-spin 5-coordinate iron(II) porphyrin models of oxygen binding proteins.[20b,c] The four N atoms of the cyclam cap are coplanar to within 0.12 Å, and their least-squares mean plane is within 0.9° of being parallel to the least-squares mean plane through the four pyrrole nitrogens. The 24 carbon and nitrogen atoms of the porphyrin core are coplanar to within 0.21 Å; this 24-atom core is pseudo-S_4-ruffled and within 0.5° of being parallel to the two N_4 groupings of the porphyrin and cyclam moieties. The mean planes of the 24-atom porphyrin core and the 14-atom cyclam cap are separated by 4.05 Å and within 0.4° of being parallel. The bond lengths and angles presented in Table 2 reveal the presence of highly precise, but otherwise unexceptional, metrical parameters for the capped porphyrin ligand of **7**.

An examination of nitrogen−nitrogen separations for the cyclam cap of **7** is informative. The two pairs of unique nitrogen−nitrogen separations in the cyclam cap which correspond to n values of 2 and 3 for the $N-(CH_2)_n-N$ chains, average 3.83 (4, 0, 0, 2) and 4.93 (6, 3, 3, 2) Å, respectively. These values can be compared with values of 3.68 and 4.94 Å which can be calculated for these same nitrogen−nitrogen separations assuming totally extended $N-(CH_2)_n-N$ chains in the cap with tetrahedral carbons and C−N and C−C bond lengths of 1.48 and 1.54 Å, respectively. These nitrogen−nitrogen separations indicate a highly stretched conformation for the cyclam cap which places the four nitrogens as far as possible away from each other and as far as possible from the pseudo-C_2 axis of the molecule. The slightly longer observed nitrogen−nitrogen separation for the $n = 2$ chains is the result of angles at the carbons which are slightly larger than the idealized tetrahedral value.

The steric requirements of attaching the cyclam cap to the four *N*-phenylacrylamide bridges from the methine carbons are partially responsible for this stretched conformation, but another factor appears to be the formation of hydrogen bonds (Table 3) in these bridges. The amide N−H bond in each of the acrylamide bridges is pointed at the lone pair of the nearest cyclam nitrogen. The four (amide)N···N(amine) separations range from 2.80 to 3.01 Å, and the (amide)N−H···N(amine) angles range from 142° to 149°. Each amide nitrogen is coplanar (to within 0.07 Å) with the three atoms covalently bonded to it as well as the hydrogen-bonded cyclam nitrogen. These hydrogen bonds produce a kink in each of the acrylamide links to the cyclam cap. While hydrogen-bonded in this manner, these acrylamide links are less flexible, and the distance which they can span is reduced. The net effect of these hydrogen bonds is to "stretch" the easily deformed cyclam cap radially away from the pseudo-C_2 axis, thereby providing maximal separation between the "linked" amine nitrogens in the cap; they

(21) The symbol N_p is used to designate a pyrrole nitrogen of the porphyrin core.

(22) The first number in parentheses following an average value of a bond length or angle is the root-mean-square estimated standard deviation of an individual datum. The second and third numbers are the average and maximum deviation from the average value, respectively. The fourth number represents the number of individual measurements which are included in the average value.

(23) The symbol C_t is used to represent the center of gravity for the four coordinated pyrrole nitrogens of the porphyrin core.

(24) Glick, M. D.; Cohen, G. H.; Hoard, J. L. *J. Am. Chem. Soc.* **1967**, *89*, 1996.

(25) Pauling, L. *The Nature of the Chemical Bond*, 3rd ed.; Cornell University: Ithaca, NY, 1960; p 260.

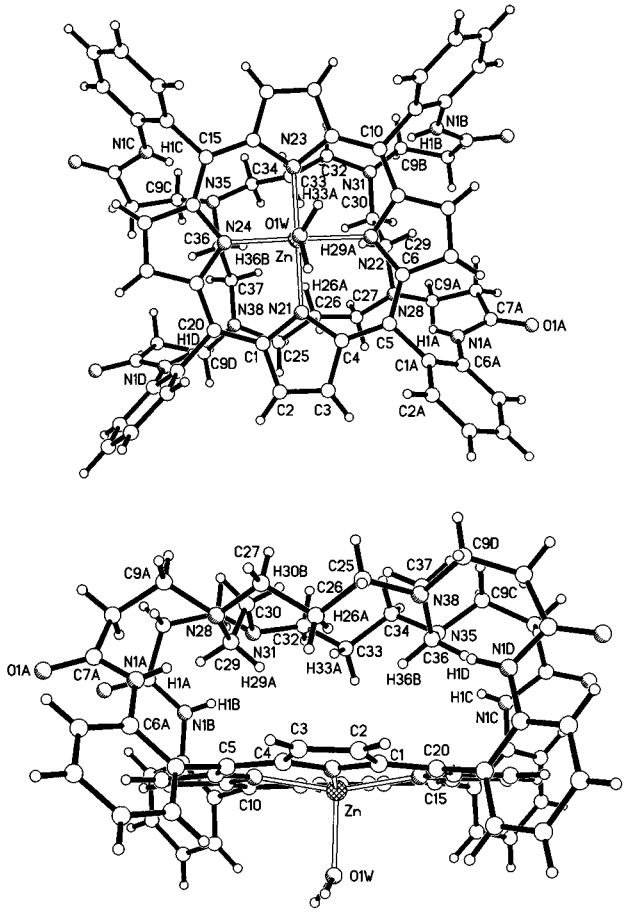

Figure 5. (a, top) Perspective drawing of the solid-state structure for the Zn(cyclam-capped porphyrin)(OH_2) molecule (**7**) present in its crystalline $H_2O/CH_3OH/CH_2Cl_2$ solvate. The Zn atom is represented by medium-sized shaded sphere, and carbon and hydrogen atoms are represented by medium-sized and small open spheres, respectively. The molecule is viewed nearly parallel to the pseudo-C_2 axis of the molecule which passes through the Zn atom and the oxygen (O_{1W}) of the coordinated water molecule. (b, bottom) Perspective drawing of the solid-state structure for the Zn(cyclam-capped porphyrin)(OH_2) molecule (**7**) present in its crystalline $H_2O/CH_3OH/CH_2Cl_2$ solvate. All atoms are represented as in (a). The molecule is viewed nearly perpendicular to the pseudo-C_2 axis of the molecule which passes through the Zn atom and the oxygen (O_{1W}) of the coordinated water molecule.

also reduce the size of the gas binding cavity on the distal side of the porphyrin by reducing the separation between the cyclam cap and the porphyrin core.

The sterically congested nature of the interior surface of the gas binding cavity in **7** can be seen from the space-filling drawing in Figure 6. Examination of a similar space-filling drawing for the interior of the gas binding cavity (with the Zn, coordinated water, and porphyrin core deleted) shows it to be roughly rectangular in shape with four "van der Waals pockets" at the ends of its diagonals near the amine nitrogens and amide protons. It also contains four cyclam methylene groups (C_{26}, C_{29}, C_{33}, and C_{36} and their hydrogens) clustered around the pseudo-C_2 axis of the molecule. One hydrogen from each of these four methylenes protrudes into the cavity and makes H···H contacts of 2.20−2.51 Å with at least two of the other three. These H···H contacts are comparable to the 2.40 Å van der Waals diameter of hydrogen[25] and are probably responsible for the reduction in molecular symmetry mentioned above. These four methylene groups would presumably have unfavorable steric interactions with a terminally-bonded CO ligand on the distal side of the porphyrin. The inability of this cavity to

Table 2. Selected Average Bond Lengths (Å) and Angles (deg)[a] Involving Non-Hydrogen Atoms in Crystalline Zn(cyclam-capped porphyrin)(OH_2) (**7**)[b,c]

parameter	value	parameter	value
	Bond Lengths (Å)		
$Zn-N_{21}$	2.069 (3, 4, 7, 4)	C_1-N_{21}	1.374 (4, 4, 8, 8)
$Zn-O_{1W}$	2.092 (3)	C_1-C_2	1.438 (5, 3, 5, 8)
C_2-C_3	1.343 (5, 1, 1, 4)	C_4-C_5	1.401 (4, 6, 11, 8)
C_5-C_{1A}	1.506 (5, 6, 7, 4)	$N_{1A}-H_{1A}$	0.81 (4, 6, 12, 4)
$C_{6A}-N_{1A}$	1.411 (5, 3, 7, 4)	$C_{7A}-N_{1A}$	1.348 (6, 14, 18, 4)
$C_{7A}-O_{1A}$	1.224 (6, 8, 16, 4)		
	Bond Angles (deg)		
$N_{21}ZnN_{22}$	88.5 (1, 9, 12, 4)	$N_{21}ZnO_{1W}$	99.3 (1, 15, 17, 4)
$N_{21}ZnN_{23}$	161.3 (1, 2, 2, 2)	$ZnN_{21}C_4$	126.2 (2, 11, 16, 8)
$N_{21}C_4C_5$	125.5 (3, 2, 5, 8)	$N_{21}C_4C_3$	109.3 (3, 2, 4, 8)
$C_3C_4C_5$	125.2 (3, 3, 6, 8)	$C_4C_5C_6$	125.5 (3, 8, 13, 4)
$C_2C_3C_4$	107.4 (3, 2, 8, 8)	$C_{2A}C_{1A}C_5$	118.8 (3, 5, 9, 4)
$C_{6A}C_{1A}C_5$	122.9 (3, 5, 6, 4)		

[a] Bond lengths and angles in the porphyrin core and *N*-phenylacrylamide links have been averaged according to the idealized C_{4v} symmetry of the "uncapped" ligand. Entries in the table are for one unique bond length or angle of each set. [b] See ref 22 for an explanation of the numbers in parentheses following each averaged value. [c] Atoms are labeled in agreement with Figure 5.

accommodate a CO which is linearly-bonded to a nearly in-plane Fe^{2+} ion can be demonstrated by making selective alterations to the structure of **7**: (1) place an Fe^{2+} ion at the center of gravity (C_t) of the four pyrrole nitrogens; (2) place the carbon and oxygen atoms of a CO ligand at distances[26] of 1.77 and 2.89 Å, respectively, away from the Fe^{2+} ion along the pseudo-C_2 axis of the molecule on the distal side of the porphyrin. Assuming no alteration in the cyclam-capped porphyrin ligand, such an arrangement produces a series of very short O···H and O···C contacts between the CO ligand and the cyclam cap on the porphyrin: O···H_{26a}, 1.38 Å; O···H_{29a}, 1.98 Å; O···H_{33a}, 1.37 Å; O···H_{36b}, 1.59 Å; O···C_{26}, 2.30 Å; O···C_{29}, 2.75 Å; O···C_{33}, 2.29 Å; O···C_{34}, 2.93 Å; O···C_{36}, 2.39 Å; and O···C_{37}, 2.80 Å. These can be compared with the van der Waals values[24] of 2.60, 3.10, and 3.40 Å for O···H, O···C, and O···methyl contacts, respectvely. Such short nonbonded contacts would obviously preclude the presence of a CO ligand which is linearly bonded to the Fe unless the conformation of the porphyrin ligand changed dramatically. Significant structural changes in the porphyrin ligand could result from a disruption of the hydrogen bonds present in the acrylamide links followed by rotations about the appropriate C−C and C−N single bonds in these links and the cyclam cap. It is not obvious that such structural alterations would increase the size of the gas binding cavity sufficiently to accommodate a CO ligand which is linearly-bonded to a nearly in-plane Fe. This cavity could obviously more easily accommodate a bent terminally-bonded O_2 ligand[20b] with an Fe−O bond length of 1.898 Å and an Fe−O−O angle of 129°.

As noted above, the gas binding cavity in **7** contains four nearly equivalent van der Waals pockets at the ends of its diagonals near the amine nitrogens and amide protons. The most favorable orientation for a bent O_2 ligand would presumably be one which directs the noncoordinated oxygen into one of these pockets. This arrangement should produce the smallest number of short O···H and O···C contacts between the O_2 ligand and the cyclam cap. Four such orientations exist for a bent O_2 ligand about the pseudo-C_2 axis of **7**; each of these places the Fe−O−O grouping near a plane which passes through opposite pairs of methine carbons and is oriented perpendicular to the porphyrin core. This also happens to be the orientation for a

(26) Peng, S. -M.; Ibers, J. A. *J. Am. Chem. Soc.* **1976**, *98*, 8032.

Table 3. Intramolecular Hydrogen-Bonding Interactions in *N*-Phenylacrylamide Links of Crystalline Zn(cyclam-cappped porphyrin)(OH_2) (**7**)[a]

donor atom (D)[b]	acceptor atom (A)	distance (Å) (D···A)	distance (Å) (H···A)	angle (deg) (D−H···A)	angle (deg) (H−D···A)	angle (deg) (H···A−X)[c]
$N_{1A}-H_{1A}$	N_{28}	2.798	2.10	149	23	83 (C_{9A}) 117 (C_{27}) 114 (C_{29})
$N_{1B}-H_{1B}$	N_{31}	2.934	2.27	142	28	79 (C_{9B}) 125 (C_{30}) 119 (C_{32})
$N_{1C}-H_{1C}$	N_{35}	2.825	2.17	149	23	84 (C_{9C}) 122 (C_{34}) 112 (C_{36})
$N_{1D}-H_{1D}$	N_{38}	3.007	2.19	146	24	80 (C_{9D}) 119 (C_{25}) 124 (C_{37})

[a] All atoms belong to the asymmetric unit for which fractional atomic coordinates are given in Tables S1 and S3 of the Supporting Information. [b] Hydrogen atoms involved in the interaction are also included. [c] The symbol X is used to designate an atom which is covalently bonded to the acceptor nitrogen atom A. The atom given in parentheses after the angle value is X.

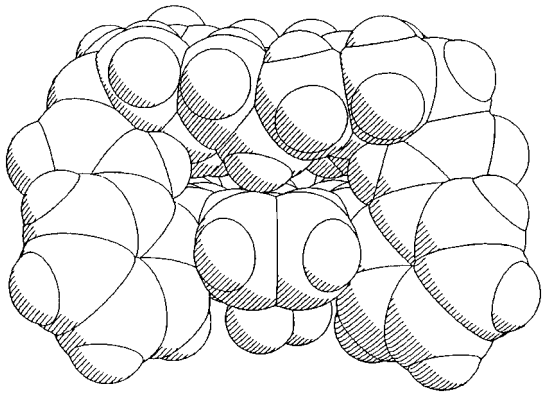

Figure 6. Space-filling drawing of the solid-state structure for the Zn(cyclam-capped porphyrin)(OH_2) molecule (**7**) present in its crystalline $H_2O/CH_3OH/CH_2Cl_2$ solvate. The molecule is viewed as in Figure 5b—nearly perpendicular to the pseudo-C_2 axis of the molecule which passes through the Zn atom and oxygen (O_{1W}) of the coordinated water molecule.

bent O_2 which minimizes nonbonded contacts between the uncomplexed oxygen of the O_2 ligand and the pyrrole nitrogens of the porphyrin core and has been observed previously[20b,c] in synthetic models of the O_2 binding site in Hb and Mb.

The ability of the gas binding cavity in the cyclam-capped porphyrin to accommodate a terminally-bonded bent O_2 ligand can also be assessed by making selective alterations to the structure of **7**: (1) place an Fe^{2+} ion at the center of gravity (C_t) of the four pyrrole nitrogens; (2) place one oxygen atom (O_{1x}) of an O_2 ligand at a distance[20b] of 1.898 Å away from the Fe^{2+} ion along the pseudo-C_2 axis of the molecule on the distal side of the porphyrin; (3) place a second oxygen atom (O_{2x}) 1.205 Å away from this (first) oxygen along the vector from the Fe-bonded oxygen atom (O_{1x}) to the cyclam nitrogen N_{31}. This arrangement produces an Fe−O−O angle of 123°, an $O_{2x}\cdots N_{31}$ separation of 2.68 Å, and a series of short O···H and O···C contacts between the O_2 ligand and the cyclam cap: $O\cdots H_{26a}$, 2.19 Å; $O\cdots H_{29a}$, 1.45 Å; $O\cdots H_{33a}$, 1.12 Å; $O\cdots H_{33b}$, 2.27 Å; $O\cdots C_{26}$, 3.03 Å; $O\cdots C_{29}$, 2.26 Å; $O\cdots C_{30}$, 2.57 Å; $O\cdots C_{32}$, 2.80 Å; $O\cdots C_{33}$, 1.99 Å; $O\cdots C_{34}$, 3.13 Å; and $O\cdots C_{36}$, 3.24 Å.

Although several of these contacts are considerably shorter than those which would be expected from summing the respective van der Waals radii,[25] they could be lengthened with considerably less ligand adjustment than those required for a linearly-bonded CO. Disrupting the hydrogen bonds in one or more of the *N*-phenylacrylamide links could cause the cyclam cap to be tilted away from the porphyrin mean plane. More specifically, disruption of the hydrogen bonds in the *N*-phenylacrylamide link to N_{31}, and presumably those to N_{28} and N_{35} as well, would allow the cyclam cap to swing away from the porphyrin core, thereby producing a substantially larger pocket inside the gas binding cavity near N_{31} and the uncomplexed oxygen atom of the O_2 ligand. Alleviating short nonbonded interactions between a (nearly) linearly-bonded CO ligand and the cyclam cap in the modified structure of **7** would, on the other hand, require a substantial movement of the cyclam cap not only away from the porphyrin mean plane but also away from the pseudo-C_2 axis. A linearly-bonded CO ligand would have its bond nearly parallel to the pseudo-C_2 axis and perpendicular to the mean planes of both the porphyrin core and the cyclam cap; its oxygen would also be pointed directly at the cyclam methylene hydrogens which protrude into the gas binding cavity near the pseudo-C_2 axis.

Reducing the number of methylene groups in either the *N*-phenylacrylamide links or the chains connecting amine nitrogens within the cyclam cap (e.g., **3**) would be expected to reduce the size of a maximally expanded gas binding cavity. Shorter acrylamide links to the cap would not be able to span the same distance as longer links when hydrogen bonding is disrupted. These shorter links would therefore produce a smaller separation between the cap and the porphyrin core when the gas binding cavity is fully expanded. Shorter methylene chains between the four amine nitrogens in the cap would stretch the *N*-phenylacrylamide links by pulling them closer to the C_2 axis; if these four links were already fully extended, the cap would again be pulled closer to the porphyrin core, producing a smaller fully expanded gas binding cavity. Either type of ligand modification would be expected to reduce the size of the van der Waals pocket(s) closest to that modification. This in turn could reduce the ability of the gas binding cavity to accommodate an O_2 ligand which is bonded in such a bent fashion to a nearly in-plane Fe^{2+}.

The above structural data and arguments are indeed borne out through experimental results, as seen revisiting Table 1. Immediately note that the *M* values are strikingly low. Some are, in fact, ca. 5 orders of magnitude lower than those reported for Hb and Mb. This observation seems to truly indicate that cavity dimensions are important. Specifically, comparison of compounds **1**, **2**, and **3** shows a tremendous decrease in CO affinity. **1** binds carbon monoxide with a $P_{1/2}(CO) = 2.9$ Torr while **2** and **3** show no CO affinity up to 1 atm.

Furthermore, the O_2 affinity of **3** is drastically lower than that of **2**. While 1,2-Me_2Im-ligated **2** yields a $P_{1/2}(O_2) = 22$ Torr at 25 °C, **3** under the same conditions yields an immeasurably low O_2 affinity. Only after decreasing the temperature to

4 °C was a $P_{1/2}(O_2) = 760$ Torr determined. The only difference in the two compounds is the cap size, the cap of **3** having two $-CH_2-$ units less than the cap of **2** ($n = 2, 2, 2, 2$ vs $n = 2, 3, 2, 3$). In following with the trend observed for CO affinities, **1** yields an increased O_2 affinity compared to **2**, and of course **3**. These trends correlate positively with increased cavity dimensions, indicating a large cavity for **1** relative to **2** and **3**.

The avid binding of O_2 to **4** and **6** was demonstrated by the lack of displacement of bound O_2 under a continuous purge with pure Ar. This is dramatically different from the reactivity of the Cu-free compounds, which showed reversible O_2 binding under the same conditions. The difference in reactivity between Cu(I) and Cu-free compounds demonstrates that the Cu(I) plays a crucial role in dioxygen binding.

The possibility of an electrostatic interaction with the lone pairs of the aza-crown ring does not seem likely since the lone pairs point away from the cavity toward the amide H and appear to be involved in hydrogen bonding according to the crystal structure of **7**. Comparison of compounds **1** and **5** with compounds **4** and **6** is instructive. Carbon monoxide affinity with and without Cu(I) provides a test as to the extent of the lone pair effects on the binding. If the lone pairs were playing a significant role in the inhibition of CO binding, the Cu-containing compounds would have greater carbon monoxide affinities, since the lone pairs of the ring are bound to a cationic metal ion. Instead the presence of the Cu slightly decreases the model's affinity for CO. However, one cannot ignore the potential steric implications of a Cu ion for the cavity. Without structural evidence, it remains unclear whether or not the Cu ion is held in a position that could add its own steric clash with a bound CO. Future X-ray studies of **1** and **4** or the corresponding Zn analogues will be required to settle this question.

Infrared spectra were also examined (compounds **1** and **4**, Table 1). The Cu(I) derivative model **4** has a CO stretch 9 cm^{-1} higher than that of the Cu-free model. This is consistent with greater CO π-back-bonding in the Cu-free complex. Back-bonding is correlated with the strength of the Fe−C bond;[10a] hence, the increased CO stretch in the Cu(I)-containing complex **4** is consistent with a more weakly bound CO molecule and a lower CO affinity. The similar CO affinity of **4**, compared with **1**, is indirect evidence that the bulky bromide ligand does not protrude into the cavity. If this were the case, the CO affinity of **4** would be much lower.

Conclusion

In conclusion we have synthesized and characterized a class of iron(II) porphyrins which show unusually low *M* values. These models are the first reported to exhibit *M* values less than 1. The *M* values are predominantly influenced by CO affinity, and experimental evidence indicates that steric interactions are responsible for the effect. This work suggests that steric effects cannot be ruled out as a major determinant of Hb and Mb CO affinity.

Acknowledgment. We thank the NIH (Grant 5R37 GM-17880-26) and the NSF (Grant CHE9123187-A4) for financial support. P.C.H. thanks the Stanford Chemistry Department for a Franklin Veatch Fellowship; B.B. thanks NATO and CNRS for a postdoctoral fellowship. We thank Dr. Charles Campana of Siemens Analytical X-ray for collection of the CCD X-ray data for **7**. We thank Dr. Miroslav Rapta for helpful discussion. We also thank the Mass Spectrometry Facility, University of California, San Francisco, supported by the NIH (Grants RR 04112 and RR 01614).

Supporting Information Available: Crystal structure report, listings of positional and thermal parameters, listings of bond lengths and angles, and perspective structural drawings for **7** (26 pages). See any current masthead for ordering and Internet access instructions.

JA963945I